The importance of atmospheric monitoring at the Pierre Auger Observatory

Bruce R. Dawson[1,⋆] for the Pierre Auger Collaboration[2,⋆⋆,⋆⋆⋆]

[1] *Department of Physics, University of Adelaide, Adelaide, S.A. 5005, Australia*
[2] *Observatorio Pierre Auger, Av. San Martín Norte 304, 5613 Malargüe, Argentina*

Abstract. The Pierre Auger Observatory is an ultra-high energy cosmic ray experiment employing a giant surface array of particle detectors together with telescopes to image fluorescence light from extensive air showers in the atmosphere. The atmosphere is the medium in which the incoming cosmic rays deposit their energy, and as a result we must monitor the characteristics of the atmosphere, including its density profile and light transmission properties, over the Observatory area of 3000 square kilometres.

1 Introduction

The challenge of understanding the origin of the highest energy cosmic rays requires an observatory with a huge area and analysis methods which minimise uncertainties in cosmic ray energy, arrival direction and mass. The Pierre Auger Observatory, located near the town of Malargüe in Mendoza Province in western Argentina, covers a ground area of 3000 square kilometres [1]. It measures the extensive air showers initiated by ultra-energetic cosmic rays with energies from around 10^{17} eV to beyond 10^{20} eV using an array of over 1600 water-Cherenkov detectors, each of 10 m^2 area and spaced on 1500 m triangular grid. During clear nights the air showers are also observed with 27 telescopes arranged in four sites around the edge of the surface detector array (figure 1). The telescopes detect the faint fluorescence light emitted by atmospheric nitrogen molecules excited by the passage of the air shower. The Observatory is thus a "hybrid" combination of two complementary techniques embodied in the Surface Detector (SD) and the Fluorescence Detector (FD).

The atmosphere is the medium in which the cosmic ray deposits its energy, and all Auger measurements by the SD and FD are influenced in some way by its properties. For example, the atmospheric density profile determines the way in which the air shower evolves with height above ground, and how the secondary particles scatter via Coulomb interactions. These things determine the shower particle density at ground level, and partly determine the lateral distribution of those particles, which in turn affects the energy estimate of the SD, $S(1000)$, the signal measured 1000 m from the shower core. In the case of the FD, the light attenuation properties of the atmosphere must be well known so that corrections can be made for an air shower that might be viewed up to 30 km from a detector.

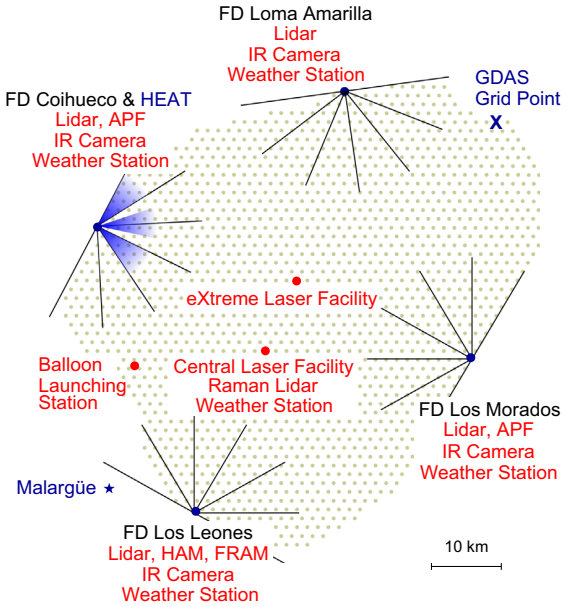

Figure 1. The Pierre Auger Observatory, showing locations of atmospheric monitoring instruments [1]. The surface detector array is indicated by the dots, and the fields of view of the fluorescence detector telescopes are indicated at each of the four FD sites.

The energy scale of the Observatory is determined using FD measurements. Fluorescence light is emitted from the shower in direct proportion to the energy deposited in the atmosphere, so the technique is intrinsically calorimetric, apart from a small correction for particles (neutrinos and high energy muons) that lose the majority of their energy in the Earth. Since the atmosphere imposes real and time-varying uncertainties on air shower measurements, Auger employs a number of atmospheric monitoring devices for characterising the properties of the atmosphere on time-scales as small as 5 minutes.

⋆e-mail: bruce.dawson@adelaide.edu.au
⋆⋆e-mail: auger_spokespersons@fnal.gov
⋆⋆⋆Author list: http://www.auger.org/archive/authors_2016_09.html

2 Atmospheric Monitoring at the Observatory

The atmospheric monitoring instruments in place at the Observatory are described in [1] and [2], and their locations are indicated in figure 1. Ground level conditions (air pressure, temperature, wind-speed, humidity etc.) are monitored every five minutes by a series of weather stations at each of the four fluorescence detector sites, and towards the center of the array at the Central Laser Facility. For more than 6 years from 2002, regular meteorological radiosonde flights were launched from the Balloon Launch Station of the Observatory to characterize the vertical atmospheric profiles of pressure, temperature and humidity, and their seasonal variations. Two laser stations, at the Central Laser Facility (CLF) [3] and the eXtreme Laser Facility (XLF), have been in operation since 2003 and 2008, respectively. They fire mJ-scale pulses of 355 nm light vertically into the atmosphere which are detected by the FDs in order to measure the aerosol content of the atmosphere hour by hour during dark periods. The CLF and XLF have been the main source of our aerosol information, but they have been augmented by elastic lidar stations at each of the FD sites [2]. Two aerosol phase-function (APF) monitors are installed at the Los Morados and Coihueco FD sites. These collimated xenon flash-bulb light sources are used to measure the angular scattering characteristics of the aerosols close to ground level [2, 4]. Optical telescopes called HAM and FRAM are used to measure the wavelength dependence of the aerosol scattering, while the FRAM is also used to examine the sky in the directions of significant air shower events to search for unusual absorption by clouds or aerosol layers [2, 5]. Infra-red cameras mounted on pan-and-tilt platforms scan the night sky for cloud, and are used to fill a database detailing the cloud obscuration in the direction of every FD pixel every 5 minutes during FD operations [6]. Finally, since November 2013 a Raman lidar system has been in operation at the Central Laser Facility. Apart from the elastic scattering receiver for the 355 nm laser light, it has channels for Raman scattering off nitrogen and water molecules [7].

Information on the vertical density, temperature and humidity profiles of the atmosphere are sourced from the Global Data Assimilation System (GDAS) described in Section 4.2 below.

3 Event Reconstruction

An overview of event reconstruction at the Auger Observatory is given in [1]. Here we provide an introduction to the features most relevant to the present topic, atmospheric monitoring.

3.1 Surface Detector Reconstruction

The primary energy of the cosmic ray is estimated with the SD using the signal 1000 m from the shower core, $S(1000)$, where the distance is measured in a plane perpendicular to the shower axis. This is determined by fitting a lateral distribution function to station signals at various distances from the shower core. Showers of a given primary energy will have a different $S(1000)$ at different zenith angles because of the attenuation of the shower size at atmospheric depths past shower maximum. This is accounted for, on average, using the method of constant intensity cuts [1], which corrects $S(1000)$ to a value it would have if the shower had arrived at a zenith angle of 38°, the median zenith angle of air showers detected by Auger in the zenith range $0 - 60°$. The relationship between this corrected measure of the shower size at ground, called S_{38}, and the primary energy E is determined using hybrid events. The near-calorimetric measurement of E by the FD calibrates the S_{38} scale for use 24-hours per day.

Two subtle effects can affect the measurement of $S(1000)$ for showers of a given energy and zenith angle. One, related to variations in pressure away from the average value, will change the atmospheric overburden and induce small changes in the shower attenuation and hence $S(1000)$. The other effect, more related to changes in the air density in the lower $\sim$ 1 km of the atmosphere, affects the Coulomb scattering of the electromagnetic portion of the air shower, and the shape of the lateral distribution function. These are small effects, contributing less than a 1% variation to the estimate of primary energy. However, when searching for weak, large scale anisotropies in the flux of cosmic rays, correcting for these effects is necessary. Such studies measure event rates above a fixed energy threshold. If that threshold energy is affected by weather effects, even small changes can result in measureable apparent anisotropies, given the steepness of the cosmic ray energy spectrum.

The collaboration has developed corrections to $S(1000)$ based on the air pressure and air density around the time of the event [8], determined using measurements at the weather stations described in Section 2. While not yet implemented in final data products like the energy spectrum (since the $< 1\%$ effect is small compared with the total systematic uncertainty on the energy scale of 14%), it is being employed in anisotropy studies such as [9].

3.2 Fluorescence Detector Reconstruction

The passage of an air shower through the atmosphere generates both fluorescence light (through the excitation of molecular nitrogen) and Cherenkov light. The Cherenkov light is much more intense, but is generally directed along the shower axis in contrast with the weaker but isotropically emitted fluorescence light. Significant amounts of Cherenkov light may be detected by the FDs if the shower axis points towards a telescope, or more commonly, when atmospheric constituents (molecules, aerosols or cloud) scatter part of the intense beam towards the FD.

The optical bandpass of the FDs is restricted to the range $300 - 400$ nm to match the spectrum of nitrogen fluorescence and to minimize the contribution of night-sky background. Within this band, absorption by atmo-

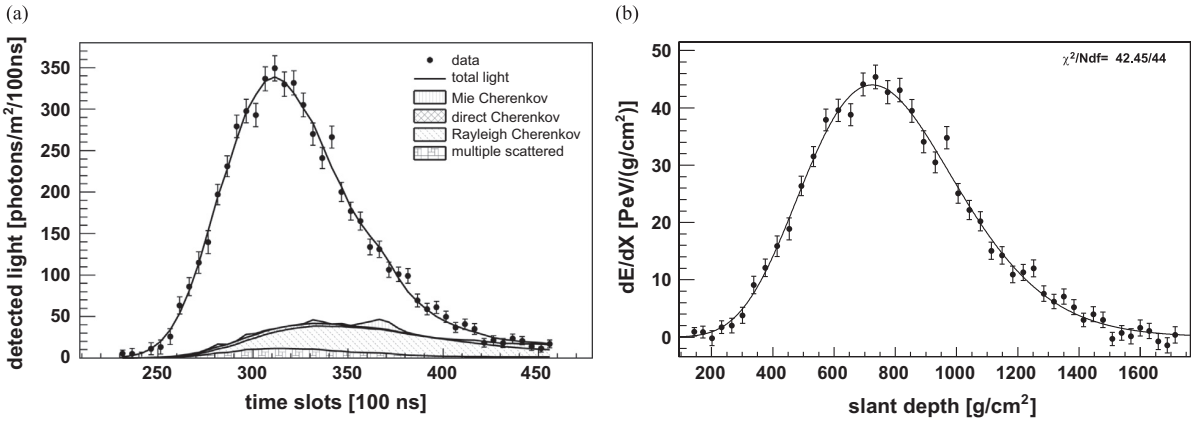

Figure 2. An example of a reconstructed shower profile. (a) The light detected at the telescope, including the fractions identified as being due to direct and scattered Cherenkov light. (b) After taking account of the shower geometry and light attenuation, application of the fluorescence efficiency gives the energy deposited along the shower track, dE/dX as a function of atmospheric depth [1].

spheric molecules is essentially zero, and light attenuation is due to scattering off molecules (Rayleigh scattering) and aerosols. One task of atmospheric monitoring is thus to understand the distribution of molecules and aerosols to account for (a) Cherenkov light scattered towards the detector, and (b) attenuation of light between the shower and the detector.

Once the detected signal is decomposed into fluorescence and Cherenkov light parts (the latter is typically less than 10%), knowledge of the atmospheric transmission will give the fluorescence light emitted from points along the observed shower track. Since the energy emitted as fluorescence light is a known fraction of the total energy deposited by the shower, our measurement yields the shower dE/dX as a function of atmospheric depth. Integrating this over depth (using a fit of the Gaisser-Hillas function, see [1] section 10.5) provides a measurement of the calorimetric energy $E_{\rm cal}$. The primary cosmic ray energy estimate is $E_{\rm cal}$ plus a small ($\sim$ 10%) correction for "invisible energy", that energy carried into the ground by high energy muons and neutrinos. The atmospheric depth at which the energy deposit maximises, $X_{\rm max}$ is also measured, an important parameter for mass composition studies. An example of a reconstructed shower profile is given in figure 2.

The atmosphere and its measurement imposes systematic uncertainties on both energy and $X_{\rm max}$. For energy, the atmosphere contributes a systematic uncertainty of about 6% at the highest energies, within the total energy systematic of 14% [1]. For the depth of shower maximum, the systematic uncertainty on $X_{\rm max}$ at the highest energies is dominated by the atmosphere and amounts to $^{+10}_{-7}$ g/cm^2 [10].

4 Examples of the Influence of the Atmosphere on FD reconstruction

Here we provide a few examples of the use of atmospheric monitoring in the analysis of fluorescence detector measurements. While the list is not comprehensive, we hope that these examples will indicate the breadth of information used to improve the quality of our analysis.

4.1 Fluorescence light yield

The fluorescence light emission from air showers is quite weak, especially compared with the Cherenkov light production, but it has the key advantage of being emitted isotropically. Very roughly, 4 photons are emitted from excited nitrogen per metre of track of a charged shower particle (and approximately independent of height), or in energy terms, about 10^{-5} of the ionization energy loss of the air shower particles is emitted as light. The emission efficiency is approximately constant through the troposphere due to the competition between excitation of the nitrogen (larger when the air density is higher) and collisional deexcitation (also higher at higher density) [11]. Molecules excited by the air shower can be quenched through collisions with nitrogen, oxygen or water vapour. For precise expectations of the light yield, the excitation and quenching processes must be well understood. For quenching, important parameters include the temperature and the partial pressures of the quenching species.

Over the past decade great advances have been made in laboratory measurements of the process, particularly by the AIRFLY Collaboration [12]. Measurements have included the precise spectral shape and intensity of emission between 300 and 400 nm, and the pressure, temperature and humidity dependence for each vibrational band within the spectrum. The temperature variation includes the expected dependence on $\sqrt{T}$ related to the probability of collisions, but also includes the more complex dependence of the quenching cross-sections on temperature.

In air shower analysis we make use of the GDAS three-hourly atmospheric profiles of pressure, temperature and humidity versus height (see next section). Together with the AIRFLY measurements, we are able to predict the absolute fluorescence yield with a systematic uncertainty of only 3.4% in the 337 nm band under standard atmospheric conditions, with an additional 1.1% systematic related to

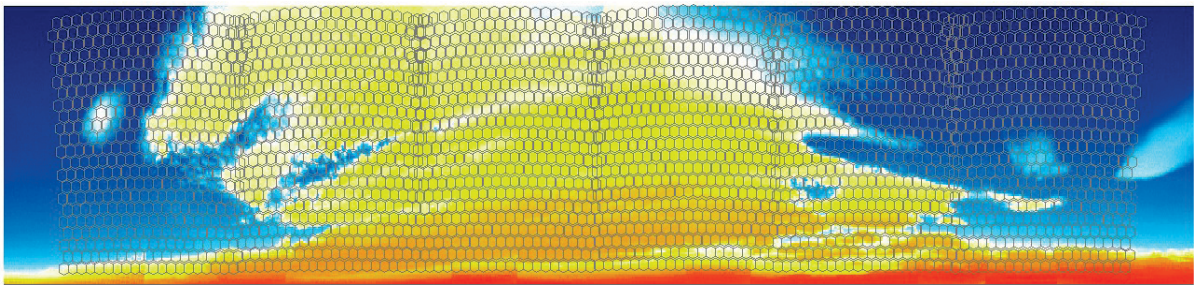

Figure 3. An example of an infra-red cloud camera image of the field of view of a fluorescence detector site. The warmer cloud is clearly visible against the colder clear night sky. Overlaid is the pattern of FD pixel fields of view for the six telescopes at this site, covering 180° in azimuth and approximately 30° in elevation. The database used in shower analysis contains an index indicating cloud coverage for every FD pixel, updated every 5 minutes during the night.

the spectrum across the entire band and our ability to account for the quenching [1].

4.2 Vertical Profiles of Density, Temperature and Water Vapour

Knowledge of the atmospheric conditions as a function of height within the troposphere is required for a number of analysis tasks. We have already described their use in accounting for the fluorescence yield. The vertical density profile is also used to convert height of a point on the shower track (from the geometrical reconstruction of the shower) into slant depth X (in g/cm^2), and in the calculation of Rayleigh scattering transmission from the shower to the detector.

For a period of six years from 2002-2008 the Auger Observatory undertook a comprehensive campaign of radiosonde balloon launches at the site to characterise the seasonal dependence of the vertical atmospheric profiles, resulting in local monthly models of air density, temperature and humidity. More recently we have switched to using data from the Global Data Assimilation System (GDAS), available since the beginning of 2005. GDAS provides information on the density, temperature and humidity profiles every three hours at points on the globe separated by 1 degree in latitude and longitude, including a point near the north-east boundary of the Auger Observatory, see figure 1. Auger has used its long-term radiosonde measurements to validate the coincident GDAS profiles [13]. Typically there is agreement to within 1 degree in temperature, 0.5 hPa in pressure, and 0.3 hPa in water vapour pressure at all relevant heights. GDAS thus provides profiles of sufficient accuracy every three hours, much more frequently than would be possible with any local radiosonde campaign.

4.3 Cloud Detection

The transmission of fluorescence and Cherenkov light from the shower to the detector can be affected by molecular and aerosol scattering, and by cloud. The effect of ozone absorption below 300 nm is negligible because of the FD optical bandpass filters have essentially no transmission at the relevant wavelengths. We have described above how GDAS density profiles are used to determine Rayleigh attenuation, and the next section will detail our aerosol measurements. Here we outline the several ways cloud is monitored.

The CLF and XLF laser facilities are the primary instruments for aerosol measurements but a by-product of that analysis is the minimum cloud-base height every hour. In addition, scanning elastic lidar stations at each of the four FD sites have been used to provide cloud height and cloud optical depth in a 45° cone in the vicinity of those sites on an hourly basis. Data from both the CLF/XLF and elastic lidars are accessed during shower analysis via calls to custom MySQL databases.

Complementary information is provided by scanning infra-red cameras, again one per FD site, which image the FD telescope fields of view (FOV) every 5 minutes and the entire sky every 15 minutes. In 2013 the cameras, having been in operation since 2002, were updated to new models with better stability and sensitivity [6]. The Gobi-384 uncooled microbolometer array cameras operate in the 8-14 μm range, and automatically scan the sky on pan-and-tilt platforms. They are radiometric cameras, meaning that they measure an absolute infra-red brightness temperature, allowing us to distinguish between warm cloud and cold clear night sky. The full-sky images are used for FD operator information, and the FOV images are processed for another MySQL database used in shower analysis, where a cloud cover index is listed for every FD pixel, updated every 5 minutes. Figure 3 shows an example FOV scan overlaid with the FD pixel pattern from one FD site.

We also access data from the GOES-12 and GOES-13 satellites for a broad overview of the cloud conditions above the Observatory [6]. A database is maintained with cloud probability maps derived from the satellite data twice per hour, with spatial resolution of 2.4 km by 5.5 km. The quality of this information has been validated by our ground based measurements [14].

Finally, the FRAM telescope scans the tracks of interesting air showers soon after observation to check for cloud and aerosols [5].

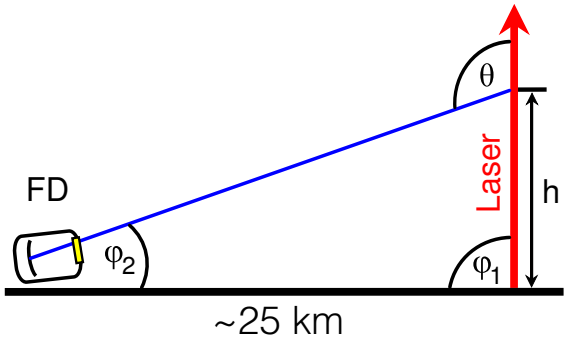

Figure 4. A sketch of the arrangement for CLF/XLF measurements of vertical aerosol optical depth, VAOD.

4.4 Aerosol Characterisation

Molecular, or Rayleigh, scattering is a more significant attenuation process than aerosol scattering. The molecular vertical optical depth between ground level and an altitude of 5 km is about 0.23 at 350 nm. This compares with an average value for the aerosol vertical optical depth of about 0.05 to the same height. However, the molecular atmosphere is much more stable than the aerosol one, and we have shown that the GDAS description of the molecular atmosphere is perfectly adequate. The challenge is to monitor the aerosol concentrations locally at the Observatory, and on time scales of an hour or less.

Our primary techniques use the Central Laser Facility (CLF) and the eXtreme Laser Facility (XLF) as part of a "bistatic" lidar for which the receiving optics are the FD stations (figure 4). In the past, cross-checks of the aerosol content have been provided by the standard elastic lidar stations at the FD sites. More recently, the FRAM telescope is contributing with aerosol estimates along the axes of interesting shower events [1, 7]. Finally, the "industry standard" technique, a Raman lidar, has been operating at the CLF site since November 2013.

The CLF and XLF lasers are frequency-tripled YAG lasers which shoot 6 mJ pulses of 355 nm light vertically into the sky [3]. (They are also steerable for other important tests, not described here). We use two approaches to measure the aerosol optical depth on an hourly basis using the CLF and XLF lasers. Both approaches make the assumption that there exists, from time to time, an aerosol-free atmosphere. We call this a "reference night".

The first approach, known as the Data Normalised (DN) method, makes direct use of hourly-averaged received light profiles on the reference night, and during the hour of interest. Examples are shown in the left-hand plot of figure 5. Each light profile is the average of 200 shots from a given hour (4 groups of 50 shots every 15 minutes), and normalised to a laser pulse energy of 1 mJ. The "bumps" in the profiles come from the imperfect light collection in the gaps between pixels in the FD camera.

When the laser pulse is shot vertically, portions of the light are scattered in the direction of the FD from all heights. The laser light suffers attenuation while travelling vertically above the laser, and in the path from the laser to the detector. By comparing the profile in a given hour to one from the reference night (where we assume that the only attenuation process is Rayleigh scattering) we can obtain (using an analytic expression [3], and taking care with possible cloud contamination) the vertical aerosol optical depth (VAOD) as a function of height, VAOD(h). An example is shown in the right-hand plot of figure 5.

This process is repeated for all four FD stations viewing either the CLF or the XLF (typically the XLF for the northerly Loma Amarilla detector), and the VAOD(h) data is loaded into a MySQL database for use during shower reconstruction. The VAODs derived within the same hour using different combinations of laser and detector site are consistent within uncertainties [3], implying near-uniform aerosol conditions across the Observatory at a given time. With the aid of the database of VAOD(h), and the horizontally-uniform aerosol assumption, the shower analysis can calculate the aerosol attenuation between any two points in space.

The DN method fills the majority of hours in the aerosol database. For hours where the DN fails for some reason, holes are filled with the alternate Laser Simulation (LS) analysis. As the name implies, we simulate the received signals from the CLF or XLF under a variety of aerosol conditions, and use this library of simulations to find the best match with a real hourly profile. For technical reasons (accounting for systematics in the laser simulation) a clean reference night is also used in this method. The DN and LS results for many hours have been compared and found to be consistent [3].

4.5 Cross-checks

In many ways the Auger Observatory's success rests on its demonstrated ability to cross-check results with different instruments or methods. Central to this philosophy is the hybrid nature of the entire Observatory, where (during dark periods) air showers are measured independently by the SD and the FD, detectors with completely different views of the showers and, largely, very different systematic uncertainties.

Much of this philosophy enters the atmospheric monitoring sphere, as may be obvious in the discussion above of various instruments used to measure cloud and aerosols. Partly, this is necessary to take advantage of the sensitivities of different instruments in different regions of phase space, but often cross-checks of the fidelity of data are also possible.

A recent example is the installation of a Raman lidar detection system using the CLF laser. The Raman technique allows an unambiguous solution to the lidar equation for aerosols by detecting inelastic backscatter from (in this case) nitrogen and water vapour [7]. The technique also has the advantage that there are standard quality assurance checks on such systems defined by experts in aerosol measurements around the world, leading to confidence in its results. On the other hand, using such a lidar in the clean aerosol environment of western Argentina is a very different situation to the majority of Raman systems located in urban settings. Work continues to validate the

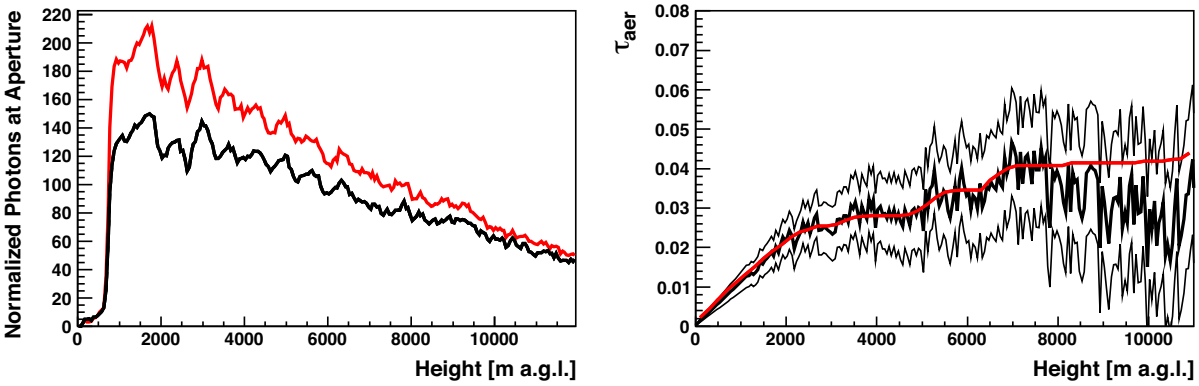

Figure 5. Left: laser profiles received at the fluorescence detector, normalised to a laser pulse energy of 1 mJ, and derived from 200 pulses over 1 hour. In red is the profile from the reference night, assumed to be aerosol free, with the black profile measured in the hour of interest. Right: the derived VAOD as a function of height above ground level, using the DN method. The central noisy line is the initial estimate of VAOD. A smoothed fit (red line) is also shown, derived with the constraint that the VAOD, being an integral quantity, cannot decrease with increasing height. Two other lines show the range of uncertainty in the VAOD [3].

standard Auger methods of aerosol characterisation using the Raman system, with three 12 minute Raman integrations per night (before and after nightly FD runs, and one integration in the middle of observations).

Finally, it is worth mentioning that shower data themselves offer scope for cross-checks of atmospheric measurements, particularly those related to aerosol transmission. Examples include comparing reconstructed energies for "stereo" views of air showers, those events seen by two, three or four FD sites, usually at different distances and aerosol transmissions. Similarly, even a single FD site energy estimate can be compared with the SD energy estimator to search for systematics related to aerosol transmission.

5 Conclusions

The monitoring of the important aspects of the atmosphere over the Pierre Auger Observatory's area of 3000 square kilometres is achieved with a suite of local instruments, and access to external data from radiosonde networks and satellites. A certain level of redundancy in the measurements is tolerated, and indeed welcomed for cross-checks. Creative uses of air-shower data has also been useful in understanding systematic issues in atmospheric monitoring. The Observatory is now embarking on a new upgrade, AugerPrime [15], with an emphasis on better SD measurements of mass-sensitive parameters, and an extension of FD operations into periods of increased night-sky brightness. Atmospheric monitoring will continue to have an important role in this new phase of the life of the Observatory.

References

[1] A. Aab et al. [The Pierre Auger Collaboration], Nucl. Instrum. Meth. **A798** 172–213 (2015).
[2] J. Abraham et al. [The Pierre Auger Collaboration], Astropart. Phys. **33** 108–129 (2010).
[3] P. Abreu et al. [The Pierre Auger Collaboration], JINST **8** P04009 (2013).
[4] S.Y. BenZvi et al., Astropart. Phys. **28** 312–320 (2007).
[5] J. Blazek et al., "Searching for Anomalous Shower Profiles with FRAM", and J. Ebr et al., "Aerosol measurements with FRAM telescopes", this meeting (2016).
[6] J. Chirinos et al., in "The Pierre Auger Observatory: Contributions to the 33rd International Cosmic Ray Conference (ICRC)", Rio de Janeiro, Brazil, 108–111 (2013) (arXiv:1307.5059).
[7] C. Medina et al., in "The Pierre Auger Observatory: Contributions to the 34th International Cosmic Ray Conference (ICRC 2015)", 127–130 (2015) (arXiv:1509.03732).
[8] J. Abraham et al. [The Pierre Auger Collaboration], Astropart. Phys. **32** 89–99 (2009).
[9] A. Aab et al. [The Pierre Auger Collaboration], Ap.J. **802** 111–121 (2015).
[10] A. Aab et al. [The Pierre Auger Collaboration], Phys. Rev. D **90** 122005 (2014).
[11] F. Kakimoto et al., Nucl. Instrum. Meth. **A372** 527–533 (1996).
[12] M. Ave et al. [AIRFLY Collaboration], Nucl. Instrum. Meth. **A597** 41–54 (2008); M. Ave et al. [AIRFLY Collaboration], Astropart. Phys. **42** 90–102 (2013).
[13] P. Abreu et al. [The Pierre Auger Collaboration], Astropart. Phys. **35** 591-607 (2012).
[14] P. Abreu et al. [The Pierre Auger Collaboration], Astropart. Phys.**50-52** 92–101 (2013).
[15] A. Aab et al. [The Pierre Auger Collaboration], "The Pierre Auger Observatory Upgrade AugerPrime" (2016) (arXiv:1604.03637).